RESEARCH ARTICLE | JULY 15 1975

Magnetic circular dichroism in hemoglobin

J. I. Treu; J. J. Hopfield

J. Chem. Phys. 63, 613–623 (1975)
https://doi.org/10.1063/1.431380

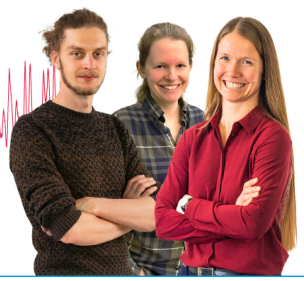

Magnetic circular dichroism in hemoglobin*

J. I. Treu† and J. J. Hopfield

Joseph Henry Laboratory, Princeton University, Princeton, New Jersey 08540
(Received 23 May 1974)

Magnetic circular dichroism (MCD) and absorption have been measured in various derivatives of hemoglobin in an applied field of 16 kG at temperatures ranging from 77 to 294°K. The visible and Soret bands have been studied. We develop a spin–orbit coupling model to help explain the sign, magnitude, and $1/T$ temperature dependence of the MCD of deoxyhemoglobin. The results for deoxyhemoglobin are compared with those for unligated separated alpha and beta chains. Differences in spectra occur which can only be attributed to the different temperature dependent heme environments for chains and for tetramers. Cyanomethemoglobin and oxyhemoglobin are also discussed.

Much recent work on hemoglobin has been concerned with mechanisms for cooperative binding of oxygen, i.e., the Koshland sequential model[1] or the Monod–Wyman–Changaux model (MWC).[2] There is considerable evidence that it is the quaternary structure, not the degree of ligation, that determines affinity, as predicted by MWC.[1–6] Furthermore, there are significant tertiary changes in each subunit upon ligation.[7–10]

With the knowledge of these configurational changes associated with cooperativity, one still must ask where it is in the molecule that the difference of free energy of binding between the first oxygen and the fourth (about 3.3 kcal/mole) is stored. Some have proposed[11] that the energy is stored in specific salt bridges at the terminal ends of the chains. Another point of view which has been expanded by one of us[12] is that the free energy is stored in a distributed fashion throughout a large portion of the protein.

Magnetic circular dichroism offers the opportunity to study the electronic structure of the heme region, as a function of the conformation of the rest of the protein. The data reported here contribute to the understanding of the changes in the heme and heme environment between two types of unligated hemoglobins, namely deoxyhemoglobin (A) and deoxygenated isolated alpha and beta chains. The NMR and EPR studies have given no details of what is happening in the unligated case. MCD and magnetic optical rotation experiments have been conducted on some derivatives of hemoglobin.[13–19] The work reported here involves temperature studies to −196 °C and new theoretical analysis of the data.

The experiment consisted of measuring the difference between the molar extinction coefficients for right and left circularly polarized light, while the sample of hemoglobin solution was located in a 16 kG. magnetic field, oriented parallel to the beam of light. Studies were conducted using wavelengths of light from 3500 to 6200 Å.

I. EXPERIMENTAL TECHNIQUE

We used the high frequency polarization modulation technique of Schnatterly and Jasperson[20] and its subsequent improvements which are described in detail elsewhere.[21,22]

The optical density difference ΔO. D. was found by averaging the observed signal for applied magnetic fields of normal and reversed polarity, to eliminate field-independent circular dichroism. From this was subtracted the similar average baseline signal with only the sample cuvette filled with buffer in the system. This corrected for field-dependent signals arising from residual phase shifts and polarizations in the optical elements, coupled with Faraday rotation in the materials situated in the magnet.

The concentrations of the samples were determined by measuring the total optical density, O. D., of the sample in zero applied field. The concentrations were calculated from published values of the extinction coefficients for the respective compounds.[23] The absorption measurements were carried out in the same optical system used for the MCD, but adapted for absorption work as described elsewhere.[24] The accuracy of this spectrophotometer was determined to be ±0.03 absorption units.

A nitrogen gas-cooled sample holder was used to accurately position the quartz cuvette containing the sample solutions in the magnet. A temperature bath of ice water or dry ice-acetone mixture regulated the temperature of the samples, and data was taken in two temperature regimes, namely approximately 8 °C, and approximately −65 °C.

Sample-handling technique at −196 °C was also developed. Most solutions of hemoglobin in water or even our low temperature buffer containing ethylene glycol described below will develop cracks when cooled to this temperature. It was determined that one of the chief causes of cracks is the constraining nature of the liquid-quartz boundary. The liquid at the interface is forced to contract with the quartz cuvette whereas the interior of the liquid contracts in a manner characteristic of itself. It may be possible to accurately match these two thermal contraction rates using a particular buffer mixture, but this can be a tedious proposition.

We employed a method which permitted the liquid to contract with a minimum of surface constraints. A strip of black plastic approximately 0.006 in. thick by $\frac{5}{16}$ in. wide was fastened to a holder so that it could be lowered into a nitrogen Dewar. The Dewar was provided with a special tail section to allow optics to be done through the Dewar. A round hold 0.1 in. in diameter was punched in the plastic. When the hole was filled with a drop of

sample solution, it was found that this drop could be frozen to −196 °C with no cracks forming. We measured the phase shift between two perpendicular components of light through several of these drops and the largest observed value was 0.1 rad, which gives rise to very small errors in the observed MCD values. A measured amount of sample was used to form the drop each time, and a collecting lens positioned after the sample in the optical system to provide more consistent results.

II. SAMPLES

Hemoglobin samples were prepared from fresh human blood at the Bell Telephone Laboratories, Murray Hill, New Jersey. The red cells were separated from the blood plasma by spinning the whole blood for approximately 10 min at 5000 rpm, washing successively with 0.9% aqueous solution of NaCl and repeating the spinning. The cells were then lysed, and the hemoglobin separated from the cellular debris by centrifuging at 15 000 rpm and washing with 4 *M* NaCl. Purification of the hemoglobin was accomplished by passing it through a Sephaex column at *p*H 7 in potassium phosphate buffer. The product was oxyhemoglobin, determined spectrophotometrically. In the preparation of deoxyhemoglobin, sodium dithionite was used as a final step after most of the bound oxygen was removed by flushing with nitrogen. The method of preparing isolated hemoglobin chains was that of Bucci and Fronticelli[25] and described in detail by Antonini.[26] The chains produced by this method have their SH groups blocked by PMB; our samples were treated to remove the bound PMB.

The concentrations of the samples were 50–60 μM in heme. They were buffered in 40 mM phosphate buffer for *p*H 6.5–7.5, and borate for *p*H 9. Because measurements were needed at low temperatures, buffers were prepared using 70% ethylene glycol ($HOCH_2CH_2OH$), 30% doubly-distilled water. No significant spectral changes were seen in switching from a water buffer to this ethylene glycol buffer.

III. THEORY

Several approaches to an understanding of the electronic structure of porphyrins have been taken over the years. Simpson[27] introduced his free-electron model in 1949, and Longuet–Higgins investigated one-electron LCAO molecular orbitals in 1950.[28] More recently, Gouterman[29–35] has applied extended Hückel theory to various porphyrins. Furthermore, an extensive analysis of MCD has been made by Stephens[36,37] and Sutherland.[38]

Stephens develops the general result that an MCD spectrum contains components due to (1) the Zeeman splitting of the absorption band (*A* terms) which have the shape of the derivative of the absorption band in the rigid shift approximation; (2) the action of the magnetic field in mixing different excited states, each having a particular magnetic moment (*B* terms), which have the shape of the absorption band itself; and, (3) the thermal distribution of population among degenerate levels which make up the ground state and which are split by the applied magnetic field (*C* terms). The *C* term has a "paramagnetic" (temperature)$^{-1}$ dependence. Oxyhemoglobin, which has its ferrous iron in a spin zero state, should have only *A* and *B* terms. Deoxyhemoglobin can be expected to also have a *C* term.

The basic molecular orbital description of the porphyrin gives the optical transitions as $a_{2u} \rightarrow e_g$ and $a_{1u} \rightarrow e_g$, in D_{4h} symmetry. The excited states $(a_{2u}\, e_g)E_u$ and $(a_{1u}\, e_g)E_u$ are mixed by configuration interaction.[31] The action of an applied magnetic field is to split the doubly degenerate E_u states, giving rise to the so-called *A*-term contribution to the MCD. In addition, the field perturbs the wavefunctions, mixing the Soret, visible, and other excited states, and giving rise to a *B*-term contribution to the MCD.

In treating oxyhemoglobin, substantial understanding of the MCD spectrum can be reached in this way. However, in deoxyhemoglobin, the iron atom is in an $S = 2$ state and the MCD characteristics are strongly influenced by this spin of the iron electrons.

In the D_{4h} symmetry of the porphyrin, the iron $3d$ orbitals are split into d_{z^2}, $d_{x^2-y^2}$, d_{yz}, d_{xz}, and d_{xy} which transform as a_{1g}, b_{1g}, e_g, and b_{2g}. Furthermore, the iron $3p$ orbitals transform as a_{2u} and e_u. In forming bonds with the porphyrin ring, molecular orbitals come about that can be thought of as linear combinations of porphyrin orbitals and iron orbitals of the same symmetry. We shall write these combined orbitals as $\varphi(a_{1u})$, $\varphi(e_{g1})$, $\varphi(e_{g2})$... with subscripts *p* or *d* to denote orbitals chiefly on the porphyrin or chiefly *d* orbitals on the iron. The many-electron states are formed as Slater determinants of these orbitals. The ground state of the deoxy porphyrin is

$$\Psi_g = \underbrace{|\varphi_p(a_{1u})^2 \varphi_p(a_{2u})^2}_{\text{chiefly } S=0} \; \underbrace{\varphi_d(b_{2g})^2 \varphi_d(e_{g1}) \varphi_d(e_{g2}) \varphi_d(a_{1g}) \varphi_d(b_{1g})|}_{\text{chiefly } S=2} \tag{1}$$

which transforms like B_{2g}. The excited states are

$$\Psi_{1\,(\text{or } 1')} = \underbrace{|\varphi_p(a_{1u})^2 \varphi_p(a_{2u}) \varphi_p(e_{g1 \text{ or } 2})}_{\text{chiefly } S=0} \; \underbrace{\varphi_d(b_{2g})^2 \varphi_d(e_{g1}) \varphi_d(e_{g1}) \varphi_d(a_{1g}) \varphi_d(b_{1g})|}_{\text{chiefly } S=2} \tag{2}$$

$$\Psi_{2\,(\text{or } 2')} = \underbrace{|\varphi_p(a_{1u}) \varphi_p(a_{2u})^2 \varphi_p(e_{g1 \text{ or } 2})}_{\text{chiefly } S=0} \; \underbrace{\varphi_d(b_{2g})^2 \varphi_d(e_{g1}) \varphi_d(e_{g2}) \varphi_d(a_{1g}) \varphi_d(b_{1g})|}_{\text{chiefly } S=2} \tag{3}$$

These excited states are mixed by configuration interaction to account for the relative intensities of the Soret and visible bands. Both excited states transform as E_u. Furthermore, the spin multiplicity is that of $S=2$, so that the states are ^5E_u and will be split in first order by spin–orbit coupling.

In first order in spin–orbit coupling, the ground state of the system is fivefold spin degenerate, and the excited states for each of $\Psi_{1,1'}$ and $\Psi_{2,2'}$ split into five levels of degeneracy 2. In a technical sense, each of these five levels gives rise to a C term of the usual sort. The spin–orbit splittings are smaller than the experimental linewidth, however, so the observations are of five superposed C-type spectra. The effective Hamiltonian of the excited state is

$$H' = \mathbf{L}\cdot\mathbf{H} + 2\mathbf{S}\cdot\mathbf{H} + \lambda\,\mathbf{L}\cdot\mathbf{S}. \tag{4}$$

The first two terms are the Zeeman splitting of the level. We must analyze the problem in detail in order to deduce λ from the observed overlapping C-type spectra.

The energy shifts of the splitting can be written in terms of the good quantum numbers of the state, namely,

$$\Delta E = L_z H_z + 2S_z H_z = \pm g\,\beta_B H_z + 2S_z H_z\,. \tag{5}$$

To see the effect of $\mathcal{H}''_{s.o.} = \lambda\,\mathbf{L}\cdot\mathbf{S} = \lambda\{L_xS_x + L_yS_y + L_zS_z\}$, we note that L_x and L_y transform as E_g and L_z as A_{1g} $+A_{2g}+B_{1g}+B_{2g}$. The first order energy shifts in the excited states are given by the matrix elements $\langle E_u|\mathcal{H}''_{s.o.}|E_u\rangle$. Since the direct product $E_u\times E_u = A_{1g}$ $+A_{2g}+B_{1g}+B_{2g}$, only the component $\langle E_u|\lambda L_zS_z|E_u\rangle$ is nonzero. The resulting energy splitting is λL_zS_z. The constant λ will be some fraction of the one-electron spin–orbit coupling operator, $-(e/2mc)(\partial V(r)/\partial r)$, where e is the charge of an electron, m is the mass of an electron, and c is the speed of light. The size of the fraction reflects the amount of iron orbital in the porphyrin molecular orbital. The ground state is an orbital singlet and is not split by spin–orbit coupling.

The effect of spin–orbit splitting on the energy levels of deoxyhemoglobin is shown in Fig. 1. In zero applied field, optical transitions occur between the singlet (orbital) ground state and the doubly degenerate excited state. When the applied field is turned on, the ground state splits into five separate levels, corresponding to the five S_z values, acting under the influence of the perturbation $2\,\mathbf{S}\cdot\mathbf{H}$. The excited state splits into ten nondegenerate levels corresponding to $\pm L_z$ and $S_z = 0, \pm 1, \pm 2$. Spin–orbit interaction raises the energy of levels with positive products L_zS_z and lowers those with negative products L_zS_z. Thus, the upper manifold, corresponding to excited levels of $+L_z$ and thereby accessible by transition from the ground state by plus polarized light, is spread apart; the lower manifold, corresponding to minus polarized transitions, is compressed.

If we examine the transition energies from the ground state, noting that these optical transitions preserve the spin quantum number of the state, we see that the absorption spectrum is composed of the ten individual lines shown on the right in the figure. Lines polarized in the minus sense are shown on the left of the zero absorption line; energy is plotted upwards.

In addition to these energy considerations, the spectrum will be affected by the fact that the population density of each S_z level in the ground state will be given by a Boltzmann distribution. The relative strength of each line depicted is proportional to the relative population of the state with that particular S_z value. This thermal distribution normally gives rise to the C terms in MCD. Let us follow what effect it will have here.

In Fig. 2, we have allowed the spin–orbit splitting to

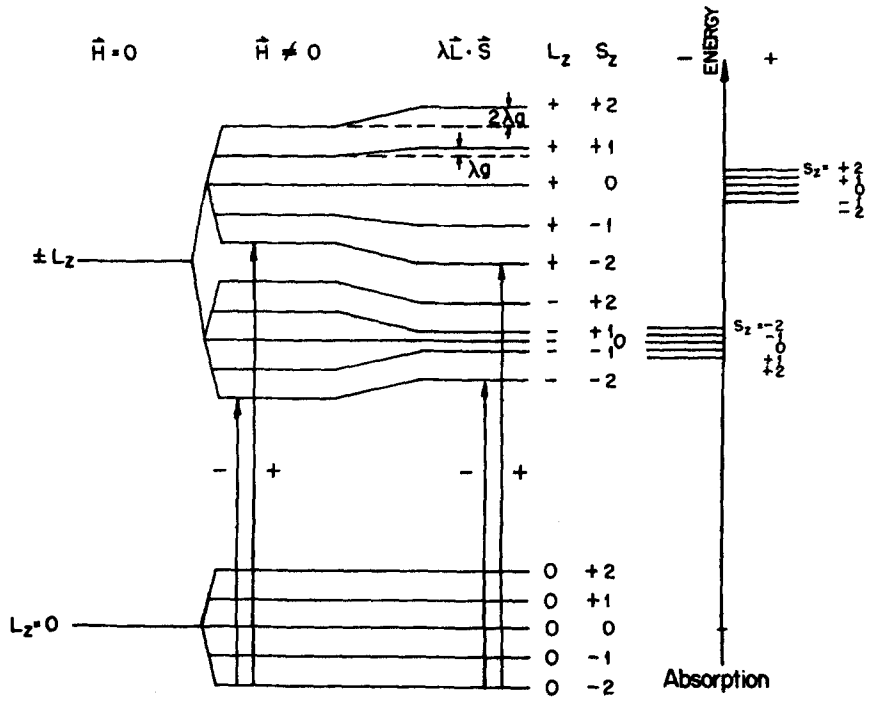

FIG. 1. Energy level scheme for product wavefunctions including the iron electrons for the case of deoxyhemoglobin ($S=2$). In an applied magnetic field, each level splits according to $H' = \mathbf{H}\cdot(\mathbf{L}+2\mathbf{S})$. Spin–orbit interaction further shifts each level according to $\lambda\mathbf{L}\cdot\mathbf{S} = \lambda L_zS_z$. The absorption spectrum is shown at the right, with plus (minus) polarized transitions shown to the right (left).

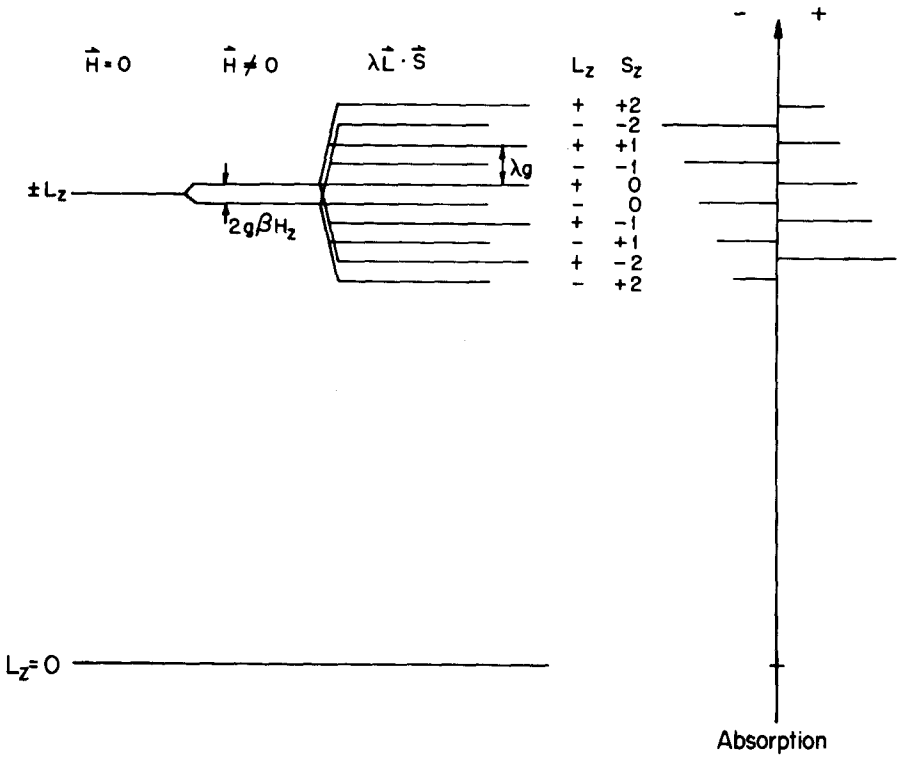

FIG. 2. The same energy level scheme as Fig. 1, redrawn with the spin–orbit splitting greater than the magnetic splitting, and the $\mathbf{H}\cdot 2\mathbf{S}$ splitting suppressed, since it occurs in both ground ground and excited states. The lines in the absorption spectrum are drawn to exaggerate intensity differences due to the Boltzmann distribution of population in the ground state.

exceed the magnetic field splitting, and we have represented the relative intensities of the lines by varying their lengths. The spin splitting of the levels has been suppressed in the level diagram for clarity. This figure shows that, for sufficiently large spin–orbit splitting, the general shape of the MCD can change from one with the plus polarized lines lying highest in energy to one in which the higher energy side of the curve is dominated by the strength of the minus polarized lines.

We have developed an expression for the differential molar extinction coefficient, $\Delta\epsilon$, for a Gaussian shaped band. Let the molar extinction coefficient for a collection of randomly oriented porphyrin molecules be written as

$$\epsilon=\epsilon(\max)\,\bar{\nu}\exp\left[-(\bar{\nu}-\bar{\nu}_0)^2/\Gamma^2\right], \tag{6}$$

where $\bar{\nu}$ is the energy of the light, $\bar{\nu}_0$ is the center of the band, and Γ is the linewidth. In an applied magnetic field, the total absorption is found as the sum of ten component bands centered at the ten energies resulting from spin–orbit splitting in the field. The difference between molar extinction coefficients is

$$\Delta\epsilon=\frac{1}{(2S+1)}\sum_{S_z}\frac{3\bar{\nu}\,\epsilon(\max)}{4}\int_{-1}^{+1}\cos\theta\exp\left[-\frac{2S_z\beta_B H\cos\theta}{kT}\right]$$
$$\times\left\{\exp\left[-\frac{(\bar{\nu}-\bar{\nu}_0-g\beta_B H\cos\theta-g\lambda S_z)^2}{\Gamma^2}\right]\right.$$
$$\left.-\exp\left[-\frac{(\bar{\nu}-\bar{\nu}_0+g\beta_B H\cos\theta+g\lambda S_z)^2}{\Gamma^2}\right]\right\}d(\cos\theta). \tag{7}$$

In this equation, the spatial average over angle θ, between the normal to the porphyrin plane and the z axis, is explicitly shown, as is the Gaussian absorption band of each of the now nondegenerate levels. An expansion is made to terms linear in $\beta_B H/\Gamma$ and in $\beta_B H/kT$. The result is

$$\frac{\Delta\epsilon}{\epsilon(\max)}=\frac{2\bar{\nu}(\bar{\nu}-\bar{\nu}_0)g\beta_B H}{(2S+1)\Gamma^2\bar{\nu}_0}\exp\left[-\frac{(\bar{\nu}-\bar{\nu}_0)^2}{\Gamma^2}\right]+\sum_{|S_z|\neq 0}\frac{\nu}{(2S+1)\bar{\nu}_0}\left(\left\{4\beta_B H\exp\left[-\frac{(\bar{\nu}-\bar{\nu}_0)^2-g^2\lambda^2S_z^2}{\Gamma^2}\right]\right\}\right.$$
$$\left.\times\left\{\frac{g}{\Gamma}(\bar{\nu}-\bar{\nu}_0)\cosh\left[\frac{2(\bar{\nu}-\bar{\nu}_0)g\lambda|S_z|}{\Gamma^2}\right]-\left(\frac{g^2\lambda}{\Gamma^2}+\frac{1}{kT}\right)|S_z|\sinh\left[\frac{2(\bar{\nu}-\bar{\nu}_0)g\lambda|S_z|}{\Gamma^2}\right]\right\}\right). \tag{8}$$

This expression is seen to be antisymmetric about $(\bar{\nu}-\bar{\nu}_0)$. This contrasts with the equation for a single C term, since the C terms are symmetrical about $(\bar{\nu}-\bar{\nu}_0)$. Our result arises from opposite contributions from slightly split simple C terms. We have left out the interband mixing in this treatment, and so there are no B terms in Eq. (8).

Some hemoglobin derivatives, e.g., HbCN, exhibit a near degeneracy in the energies of the d_{xz} and d_{yz} states

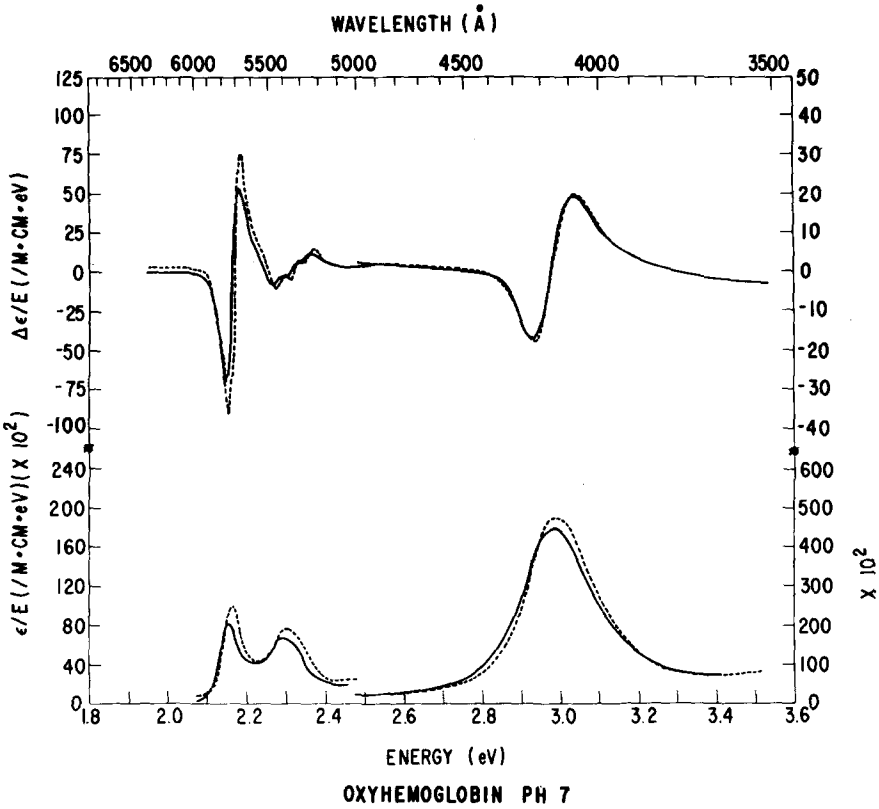

FIG. 3. $\Delta\epsilon/E$ (/M cm eV), top, and ϵ/E (/M cm eV), bottom, shown for oxyhemoglobin. Visible region is on the left and the Soret region on the right. The solid curves is the data at 8 °C; the dotted curve is data at − − 55 °C. The applied field is 16 kG.

which contain an odd number of electrons. Even in the absence of spin–orbit coupling, an orbital degeneracy in the ground state will produce a temperature-dependent MCD, namely the usual C terms. This comes because the degenerate d_{xz} and d_{yz} are mixed into states of $L_z = \pm 1$ and split by an applied magnetic field, and the lower energy state will be thermally more populated.

The shape of the broad optical absorption lines can best be understood in terms of a configuration-coordinate description, in which the probability distribution of nuclear positions causes a distribution of transition energies. Distortions which do not split x and y energy levels result in line shapes which are the same for right- and left-handed circular polarization and for the absorption line itself. Distortions which lower the symmetry and split the x-y degeneracy split the states which are mixed by the magnetic field. The MCD is depressed by such distortions, particularly far from the center of the absorption lines, and the observed MCD will not then have the shape of the derivative of the absorption line. We have carried out simple numerical calculations to investigate the effect of degeneracy-splitting dynamic distortions.

An estimate of g for oxyhemoglobin may be obtained from A terms only, in terms of the maximum values of each of $\Delta\epsilon$ and ϵ. This is

$$g \cong 1.17 \frac{\Gamma}{\beta_B H} \frac{\Delta\epsilon(\max)}{\epsilon(\max)} \quad . \tag{9}$$

In a typical example with half of the linewidth due to symmetry lowering distortions, the g value obtained by simply using Eq. (9) is only 10% too small if the line width used in Eq. (9) is the width calculated from the center of the absorption line and its peak of the MCD. This width, however, is about 30% smaller than would be expected from the optical absorption spectrum. Thus, anomalously small widths in MCD are a sign of symmetry-breaking dynamic distortions, but the g values (properly calculated) are rather little altered.

IV. RESULTS

A. Oxyhemoglobin

The experimental curves for oxyhemoglobin are shown in Fig. 3. Characteristic derivative-type MCD curves are found corresponding to the electronic absorptions in the Soret and visible regions. The sign of these MCD curves is "positive," meaning that the quantum state of higher angular momentum, which absorbs plus polarized light, is shifted to higher energy.

The Soret band MCD has been fit by least squares method to a model including A terms only and also one including both A and B terms. The least squares parameters used are shown in Table I. These values are the result of curvefitting the lower energy side of the Soret MCD curve.

The MCD curves are asymmetric with respect to the center energy $\bar{\nu}_0$, and a somewhat better fit is obtained using both A and B terms. When we curvefit the data at 8° and − 55 °C, the resulting values for g are found to be 0.40 at both temperatures. The net area under the actual data, integrating from 3510 to 5000 Å, is 14% of the total integrated area of either sign, and this is independent of temperature.

TABLE I. Values of g and bandwidth Γ for oxyhemoglobin at temperature T, obtained by least-squares curve fitting. The complete MCD curve was used in the Soret region, but only the lower energy portion was analyzed in the visible, to eliminate vibrational-band contributions.

	T (°C)	$\frac{\epsilon\ (\max)}{\bar{\nu}_0}$ ($M^{-1}\cdot cm^{-1}$ cm)	g	Γ (cm^{-1})
Oxy Soret, both sides	8	5.58	0.40	637
	−55	5.95	0.40	644
Oxy, vis. Lower energy side	8	0.949	3.2	222
	−55	1.22	3.3	230

In addition to the main features of the oxyhemoglobin absorption spectrum, there is also the band at 5400 Å which has been described as a vibrational sideband of the electronic band at 5760 Å. In the MCD, at 8 °C, this region shows a reduced signal of positive sign, with shoulders suggestive of the existence of more than one MCD curve. The data at dry ice temperature bear this out, since the shoulders resolve themselves into what appears to be at least one additional MCD curve near 5400 Å, as shown in Fig. 3.

Spiro and Strekas[39] have reported resonant Raman spectroscopy studies on oxyhemoglobin in which they identify a large number of vibrational states having an energy which would locate the side-band resulting from such states in the vicinity of 5400 Å. What is more, from the polarization of the Raman lines, they have identified the symmetry of the vibrational states as A_{2g} for some and B_{1g} or B_{2g} for others. It can be shown that those modes of symmetry representation A_{2g} exhibit a magnetic circular dichroism of the same sign as the electronic state alone; however, the B_{1g} and B_{2g} modes are characterized by a MCD signal reversed in sign from the electronic state alone.

Our data are consistent with this picture of a number of superimposed vibrational side bands in the region 5500–5200 Å. Since they contribute MCD signals of opposite sign, the overall MCD curve is reduced in magnitude from the electronic band at 5760 Å. The structure in the vibrational region sharpens at dry ice temperatures. At liquid nitrogen temperature, the structure sharpens further, but no new bands are seen.

B. Deoxyhemoglobin

The outstanding features of the deoxyhemoglobin MCD spectrum, Fig. 4, are the fact that the sign of the Soret MCD is reversed from that of oxyhemoglobin, and the reduction of the MCD strength in the visible region. This visible region shows considerable structure not evident in the broad absorption peak centered at approximately 5600 Å. There is a positive MCD curve at about 5900 Å, and another at 5600 Å, but both are highly asymmetric. This region is insensitive to temperature changes from 8 °C to dry ice temperature.

Turning our attention to the Soret band, we see a 44% increase in height of the MCD signal on the low energy side of the band, upon cooling from 8° to −65 °C. There is no corresponding change in the absorption spectrum. The width of the absorption spectrum does not change upon cooling, nor does the width of the MCD. The experiments have been matched by a calculated curve based on the spin–orbit coupling model presented earlier. We feel that the asymmetry of the Soret absorption is probably due to vibronic side bands, and we have restricted our analysis of the MCD to the lower energy side to minimize the influence of such bands. The calculated curves

TABLE II. Measured values of various parameters which describe the spectra of separated chains and deoxyhemoglobin.[a]

	Alpha chains		Beta chains		Hb (A) pH 7		Hb (A) pH 9	
	16°C	−69°C	24°C	−67°C	8°C	−65°C	7°C	−70°C
MCD peak value (Soret low energy) $\Delta\epsilon/E$ ($/M$ cm eV)	71 ± 4	90 ± 4	64 ± 4	82 ± 4	90 ± 4	130 ± 6	78 ± 4	122 ± 5
Position of MCD peak (Soret low energy) (eV; Å)	2.855 ± 0.003 4343 ± 5	2.850 ± 0.003 4351 ± 5	2.852 ± 0.003 4348 ± 5	2.850 ± 0.003 4351 ± 5	2.870 ± 0.003 4320 ± 5	2.872 ± 0.003 4317 ± 5	2.869 ± 0.003 4322 ± 5	2.870 ± 0.003 4321 ± 5
FWHM of MCD (Soret low energy) (meV; cm^{-1})	76 ± 4 613 ± 32	74 ± 4 597 ± 32	83 ± 4 669 ± 32	74 ± 4 597 ± 32	70 ± 4 565 ± 32	66 ± 4 532 ± 32	70 ± 4 565 ± 32	66 ± 4 532 ± 32
Absorption peak (Soret) ϵ/E (/mM cm eV)	44.8 ± 1.3	52.1 ± 1.16	44.4 ± 1.3	54.8 ± 1.6	51.5 ± 1.5	52.0 ± 1.6	51.2 ± 1.5	54.2 ± 1.6
FWHM of absorption peak (Soret) (meV; cm^{-1})	259 ± 35 2092 ± 280	233 ± 35 1876 ± 280	279 ± 35 2250 ± 280	207 ± 35 1669 ± 280	271 ± 35 2185 ± 280	265 ± 35 2137 ± 280	210 ± 35 1694 ± 280	204 ± 35 1645 ± 280
Peak-to-Peak of MCD feature at 5600 Å $\Delta\epsilon/E$ ($/M$ cm eV)	11.7 ± 1.1	123 ± 5	8.0 ± 1	159 ± 6	2.7 ± 1	4.0 ± 1	4.2 ± 1	6.0 ± 1

[a]For MCD, applied field was 16 kG. Limits of error are estimates of instrumental accuracy only.

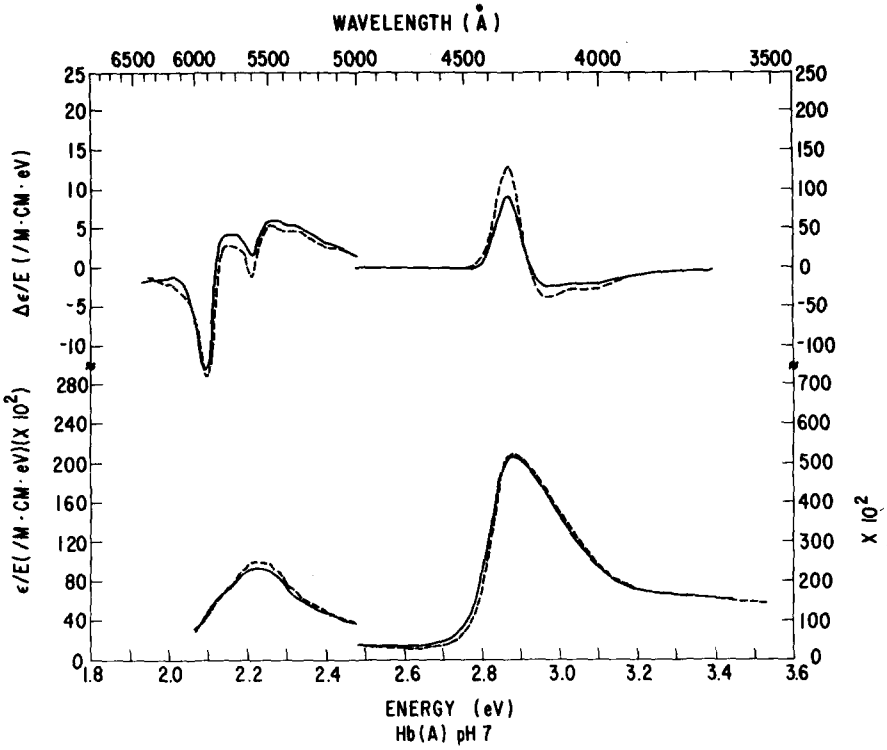

FIG. 4. $\Delta\epsilon/E$ (/M cm eV), top, and ϵ/E (/M cm eV), bottom, shown for deoxyhemoglobin pH 7. Visible region is on the left and the Soret region on the right. The solid curve is data at 8 °C; the dotted curve is data at −65 °C. The applied field is 16 kG.

based on Eq. (8) superposed on the data are shown in Fig. 5.

The three parameters g, λ, and Γ were fit using the data at both temperatures. These were fit two at a time: the 8 °C data were fit varying g and Γ; the −65 °C data were fit varying λ and Γ. This process was carried out iteratively until convergence was obtained. We set $\bar{\nu}_0 = 23645$ cm^{-1} as the zero crossing point of the MCD curve and used the absorption data to determine $\epsilon(\max)/\bar{\nu}_0 = 6.32$ M^{-1} cm^{-1} cm at $T = 8$ °C and 6.38 M^{-1} cm^{-1} cm at $T = -65$ °C. The results were $g = 0.36$, $\lambda = 271$ cm^{-1} and $\Gamma = 606$ cm^{-1}.

As a further test of the spin–orbit model and the C-term origin of the MCD, we measured the absorption and MCD of deoxyhemoglobin at $T = -196$ °C. To within the limits of error of that measurement, no better than 50%, the ratio ΔO.D.(max)/O.D.(max) behaved as expected according to Eq. (8). No additional curvefitting is implied here. Using the least squares parameters obtained above, we simply calculated what value that ratio would have at −196 °C, obtaining 7.0×10^{-3}. The experimentally obtained ratio was 6.6×10^{-3}. This behavior is shown in Fig. 6. A linear extrapolation of the temperature dependence of the ratio ΔO.D.(max)/O.D.(max) based on the data at 8° and −65 °C predicts a value of 3.8×10^{-3}.

The uncertainty in the liquid nitrogen temperature measurements comes principally from light loss by refraction at the surfaces of the sample drop. However, any loss of light will result in a larger effective O.D., and thus a smaller apparent ratio value. For this reason, we interpret the $T = -196$ °C data as consistent with the $1/T$ dependence described.

No significant differences between Hb(A) at pH 7 and pH 9 were seen. The results of curvefitting the pH 9 data are $g = 0.39$, $\lambda = 240$ cm^{-1}, and $\Gamma = 652$ cm^{-1}.

C. Separated chains

The Soret MCD in separated chains looks qualitatively the same as for Hb(A), increasing in height some 30% between 25° and −70 °C. However, the temperature dependence of the absorption band is quite different. Figures 7 and 8 display the experimental results for alpha and for beta chains, respectively. The Soret absorption band in separated chains is depressed in height by about

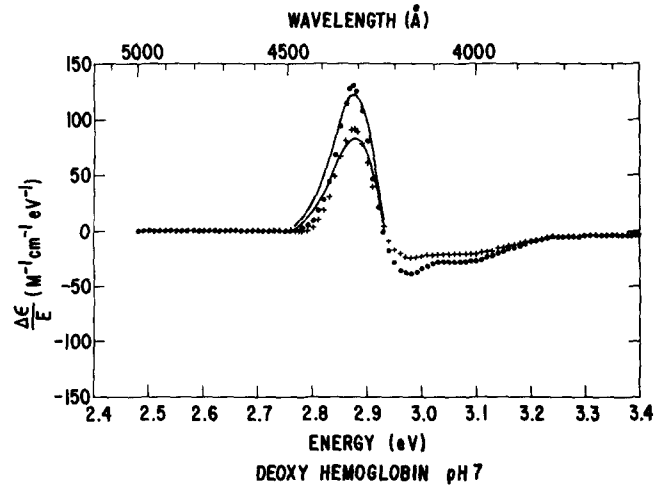

FIG. 5. Calculated curves (solid) shown together with deoxyhemoglobin Hb(A) at $T = 8$ °C (crosses) and $T = -65$ °C (dots). The calculated curves are based on Eq. (8) using the best fit values of $g = 0.36$, $\lambda = 271$ cm^{-1}, and $\Gamma = 606$ cm^{-1}. Constants used in the fitting procedure were $\bar{\nu}_0 = 23645$ cm^{-1}, $\epsilon(\max)/\bar{\nu}_0 = 6.32$ M^{-1} cm^{-1} cm, at $T = 8$ °C, and $\epsilon(\max)/\bar{\nu}_0 = 6.38$ M^{-1} cm^{-1} cm, at $T = -65$ °C.

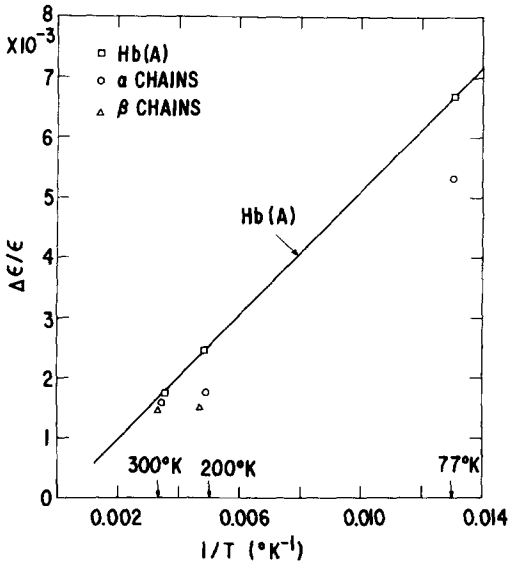

FIG. 6. Plot of the ratio ΔO. D. (max)/O. D. (max) for the low energy side of the Soret region of hemoglobin tetramer (deoxyhemoglobin) pH 7 and separated alpha chains, versus $1/T$ (/°K). If the spin–orbit interaction dominates the MCD signal, then the value of this ratio should have a $1/T$ dependence.

12% relative to Hb(A) and is somewhat broader.[40] We observed that, upon cooling, the Soret absorption narrows sharply and increases in height by approximately 27%. The picture is complicated by the observation that, while the absorption curve narrows by some 27%, the MCD curve does not change significantly in width. This contrasts with the Hb(A) case in which both absorption and MCD have constant widths over this temperature range.

Differences between Hb(A) and separated chains occur, too, in the visible region. At the warmer temperature, the chains appear the same as Hb(A), exhibiting some structure at approximately 5900 and 5600 Å. Upon cooling to − 70 °C, the feature at 5600 Å sharpens up into a well resolved peak with a height some 15 times what it is at 8 °C. In absorption, the broad visible band sharpens into two resolved peaks, at 5600 Å and approximately 5400 Å.

Furthermore, a series of resolved smaller peaks in the MCD appear between 5400 and 5100 Å. These structures, as well as the sharpening of the 5600 Å features, are common to both alpha and beta chain spectra.

We can estimate the g value of the MCD feature at 5600 Å. The peak O. D. is 0.368 for a typical sample but approximately 0. 13 of this should not be attributed to this band alone due to overlapping neighboring bands. Equation (9) is used to estimate g, using the fact that the MCD peaks occur 192 cm^{-1} apart. The result is $g = 2 \pm 0.5$, uncertainty of ~25% arising from O. D. (max). From this value, which approaches the oxyhemoglobin result of 3.3, it might be argued that the Q_{0-0} transition occurs at 5600 Å in deoxy chains. The visible band structure on the high energy side of both absorption and MCD is very likely vibrational structure similar to that observed in oxyhemoglobin.

Figure 6 shows the ratio ΔO. D./O. D. plotted versus $1/T$ for hemoglobin pH 7 and separated chains. We see that the behavior of this ratio is close to $1/T$ for Hb(A) but more complicated for chains. Between 77 °K and the higher temperatures, there is a large change paralleling that of Hb(A).

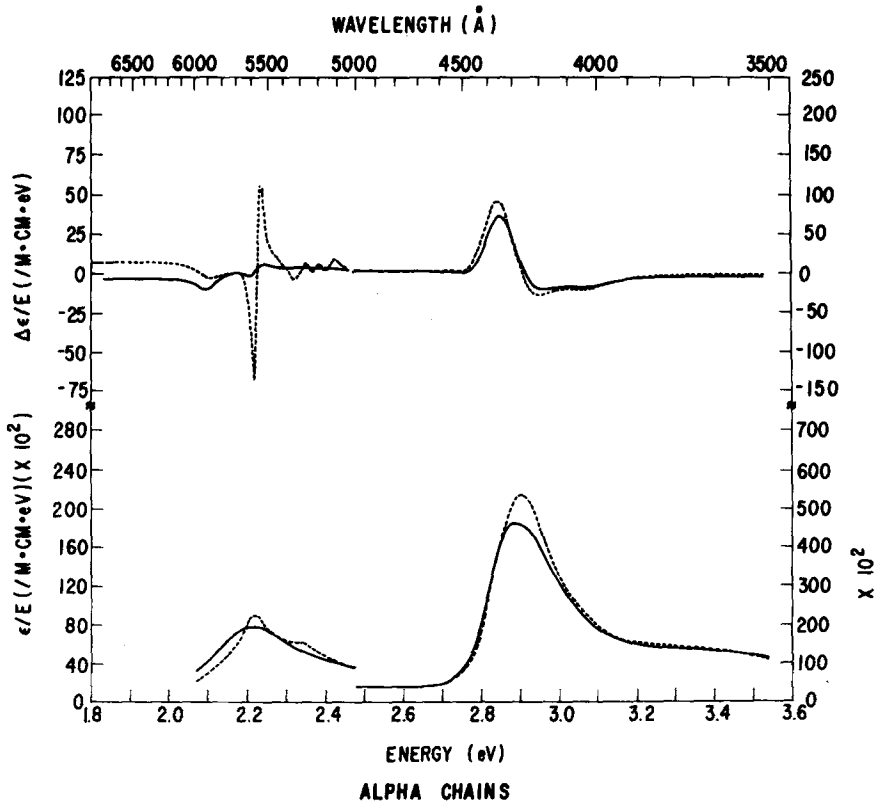

FIG. 7. $\Delta\epsilon/E$ (/M cm eV), top, and ϵ/E (/M cm eV), bottom, shown for alpha chains. Visible region is on the left and the Soret region on the right. The solid curve is data at 16 °C; the dotted curve is data at − 69 °C. The applied field is 16 kG.

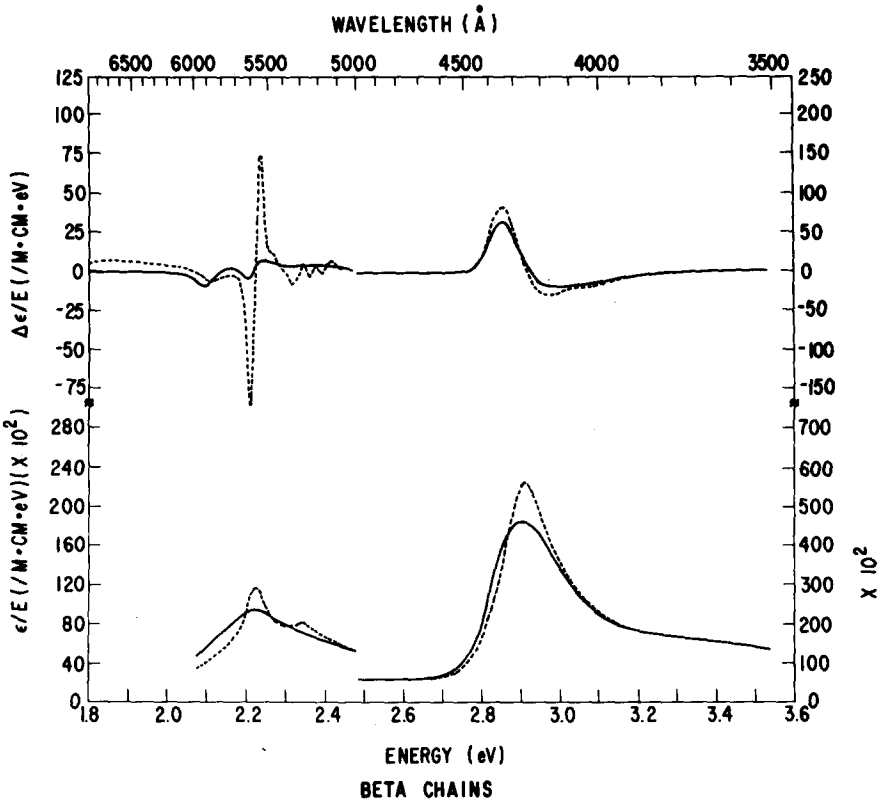

FIG. 8. $\Delta\epsilon/E$ (/M cm eV), top, and ϵ/E (/M cm eV), bottom, shown for beta chains. Visible region is on the left and the Soret region on the right. The solid curve is data at 24°C; the dotted curve is data at −67 °C. The applied field is 16 kG.

D. Cyanomethemoglobin

Cyanomethemoglobin ($S=\frac{1}{2}$) is characterized by a temperature dependent positive A-term MCD in the Soret region of greater size than oxyhemoglobin. The visible region is structured and weak. The experimental results appear in Fig. 9.

The Soret MCD is asymmetric, exhibiting a shoulder on the high energy side, near 3910 Å. The net area is small, however, amounting to between 3 and 7% of the total Soret MCD area, both at warm and cold temperatures. Thus, there is little contribution from B and C terms. Using Eq. (9), the g values are calculated to be 1.3 at 8 °C, and 2.3 at −65 °C. This calculation takes

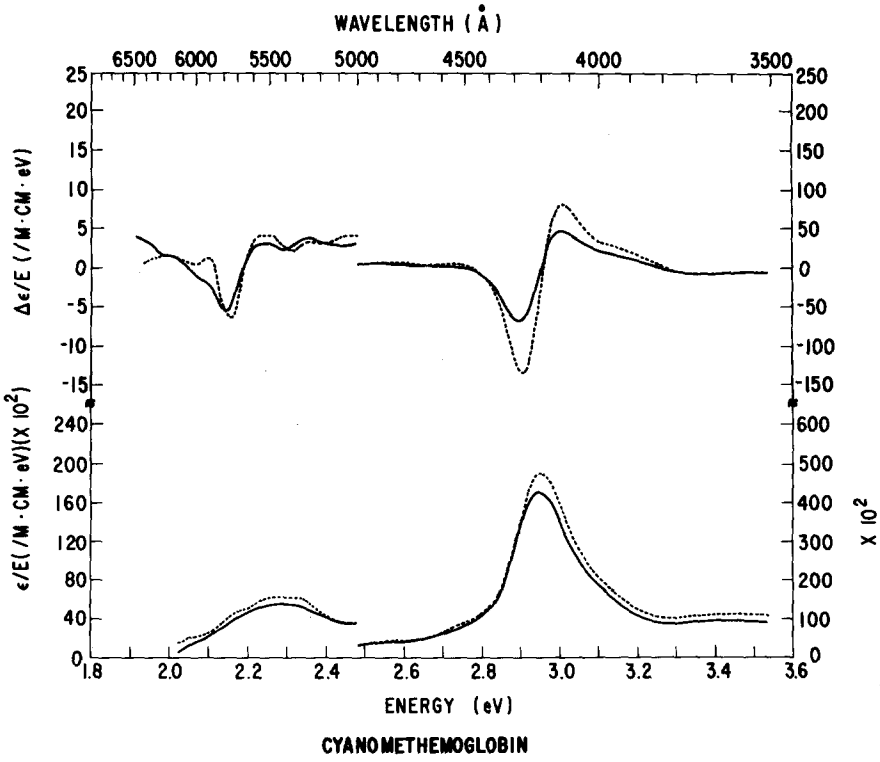

FIG. 9. $\Delta\epsilon/E$ (/M cm eV), top, and ϵ/E (/M cm eV), bottom, shown for cyanomethemoglobin. Visible region is on the left and the Soret region is on the right. The solid curve is data at 16°C; the dotted curve is data at −69°C. The applied field is 16 kG.

into account the 14% increase in absorption height upon cooling. There appears to be no appreciable narrowing of the absorption line, and so there is an increase in oscillator strength in the Soret absorption band upon cooling. This increase does not come from the visible band, which does not seem to decrease in oscillator strength.

The visible structure is complicated and weak, having a maximum strength of approximately 7 $M^{-1} \cdot cm^{-1}\ eV^{-1}$ at about 5800 Å. The visible band is relatively temperature insensitive over the temperature range studied. From the complexity of the MCD, it would seem that the visible band is composed of overlapping *pi–pi** and charge-transfer bands. Since the stronger MCD feature is seen to peak at 5800 Å, it might be thought that the *pi–pi** transition occurs in this region, to the low energy side of the absorption maximum at 5400 Å.

V. DISCUSSION

Our results for HbO_2 are qualitatively similar to those obtained by others for porphyrins. Gale[15] reports MCD measurements for a variety of octaethylporphyrins. Rein[16] and Shashoua[14] discuss the magneto-optical rotatory spectra of porphyrins, and their data can be correlated with MCD spectra. In particular, Shashoua's results for HbO_2 seem in general agreement with the present data. Malley[41] measured MCD for magnesium coprophyrin III tetramethyl ester, and found similar shaped curves to ours, except that g values were found to be 10 ± 2 essentially independent of temperature, for the Q_{O-O} transition of the visible band in the free porphyrin. We find a value of 3.2 ± 0.1. In experiments on zinc coproporphyrin I tetramethyl ester, Malley found a Q_{O-O} g value of 9.5 at room temperature and 6.4 at 77 °K. Most porphyrin derivatives exhibit Soret and visible bands with positive MCD. The comparison of the magnitude of the oxyhemoglobin values with those of the free porphyrin, the observed temperature dependence in the free porphyrin, and the asymmetric lines seen in hemoglobin all indicate that vibronic couplings will make the results in hemoglobin difficult to interpret on a quantitative basis. The expected qualitative behavior is observed in most free porphyrins and in HbO_2, with the exception of Gale's[15] data for octaethylporphyrin.

Deoxyhemoglobin (A) has an optical absorption spectrum which shows little temperature dependence and an MCD signal in the Soret which is *negative* and strongly temperature dependent. Negative MCD can come from two possible sources, "hole-like" transitions in a more than half-filled set of *pi* orbitals, and from spin–orbit coupling. Caldwell[17] treats negative MCD terms in connection with the spectrum of benzene using electron donor and electron acceptor (hole) wavefunctions based on occupied and unoccupied orbitals. Chlorophyll-a has a negative A-term shaped MCD spectrum.[14] Temperature-dependent changes in protein conformation can also lead to temperature-dependent MCD spectra, and cannot be totally ruled out as an explanation of our data. However, they would not be expected to be so spectacular, particularly at the lower temperatures. Thus, we attribute the negative MCD of the Soret band in deoxy hemoglobin to spin–orbit coupling and the superposition of C terms.

Strong temperature dependence has been observed in oxidized and reduced cytochromes by Vickery[18] and Briat.[19] The general shape of the Soret band is that of a positive but temperature-dependent A term; however, Briat analyzes the Soret MCD of cytochrome b_2 as a superposition of three separate C terms.

The presence of C terms is evidence that the iron d orbitals make significant contributions to the porphyrin *pi* orbitals. In our spin–orbit model calculation, the value of λ obtained is quite high. The value for neutral iron is 400 cm^{-1}.[42] The observed value of 270 and 240 cm^{-1} at pH 7 and pH 9, respectively, imply the transfer of the spin of 0.6 electrons from the porphyrin *pi* orbitals, or vice versa. The sign of the transfer is not determined. The value of 0.6 is large, but even in HbCN, the electron in the highest iron orbital has 0.2 of its spin delocalized onto porphyrin ring. In the present example, this transfer will be enhanced both by the fact that Fe^{2+} is involved rather than Fe^{3+}, and by the fact that in the relevant excited state, the optical excitation has moved a porphyrin electron toward the outside of the heme ring.

The MCD of deoxy chains (high affinity) and of deoxy Hb both exhibit the large "$1/T$" increase at 77 °K. The most striking difference in the behavior of chains and tetramer occurs between 8° and − 55 °C. Over this range the width of the Soret peak in the tetramer remains almost constant, while the width in the chains decreases from about 20% greater than the tetramer (at 8 °C) to the tetramer value (at − 55 °C). In spite of this decrease in the linewidth in the chains, the MCD linewidth of the chains does not change. The failure of the MCD linewidth to follow the absorption linewidth is an indication that the excess linewidth in the chains at room temperature is primarily due to symmetry-lowering distortions, (probably of a dynamic nature) capable of lifting the x-y degeneracy of the excited state. Chains also exhibited a strong MCD feature at 5600 Å and at 77 °K which the tetramer did not.

One problem with a quantitative analysis is illustrated by the fact that the zero crossing of the HbO_2 MCD curve in the Soret does not coincide in energy with the maximum of the corresponding absorption band. Furthermore, the net area of the Soret MCD curve is small (small B term). We have assumed that the zero crossing point corresponds to the center of an absorption band basically electronic in nature, and that the observed extinction coefficient for the Soret band gives the magnitude of that band. At the present level of knowledge, this is a necessary but slightly erroneous oversimplification. A full explanation of the shape of the Soret MCD, including the asymmetric nature of the absorption spectrum and the symmetries of vibronic couplings is obviously needed.

HbCN exhibited a temperature-dependent MCD of positive sign in the Soret region. HbH_2O and HbOH produced qualitatively similar results.[24] These results suggest paramagnetic contributions to the MCD. However, a temperature dependent change in the heme en-

vironment can translate itself into an increased angular momentum of the *pi* excitations and thus a T-dependent MCD. We have not studied HbCN over a temperature range sufficiently wide to prove the paramagnetic origin of the temperature dependence.

The linear strain model of cooperative binding[12] expresses the difference between the protein moiety of hemoglobin when in the R and in the T quaternary structure in terms of different temperature-dependent forces F_R and F_T of the protein acting on the heme. The Soret region shows different temperature dependences in chains and in tetramer, which could be the effect of the expected difference in the temperature dependence of the stresses on the heme in the two cases.

The spectral feature of 5600 Å is difficult to evaluate. It might be an intrinsic feature of high-affinity subunits, which could be checked in des-HIS, des-ARG Hb. It might alternatively be an artifact of some partial ligand binding to the high affinity form at low temperature. In this regard, the strong T dependence[18] of the visible band of σ-liganded ferro-cytochrome C is also of interest.

There are detectable MCD differences between high affinity and low affinity unligated subunits in the heme region. While they are visible, and although we have found the approximate size of the hybridization, the analysis is not sufficiently precise to be able to ascertain how different the iron–heme hybridization is in the two cases. The strikingly different temperature dependences of the MCD and absorption spectra shows clearly the difference in the T dependence of the two heme environments, and indicates as well a different x-y splitting perturbation in high and low affinity forms.

ACKNOWLEDGMENTS

We gratefully acknowledge the help given by Dr. Robert Shulman and Dr. Seigi Ogawa, Bell Telephone Laboratories, Murray Hill, New Jersey, for their discussions with us and the use of the facilities at Bell Laboratories. We wish to thank Miss Carmelita Castillo for her help in preparing many of the samples. Dr. Steven Schnatterly of Princeton University contributed useful information about experimental techniques.

*Supported in part by grants from NSF and the U. S. Air Force.

†Present address: General Electric Company, Research and Development Center, Schenectady, NY 12301.

[1]R. G. Shulman and S. Ogawa, Biochem., Biophys. Commun. 9, 42 (1971).
[2]R. Cassoly *et al.*, Biochem. Biophys. Res. Commun. 44, 1015 (1971).
[3]R. T. Ogata and H. M. McConnell, Cold Spring Harbor Symp. Quant. Biol. 36, 45 (1971).
[4]R. T. Ogata and H. M. McConnell, Proc. Natl. Acad. Sci. U. S. 69, 335 (1972).
[5]M. F. Perutz, Nature 237, 495 (1972).
[6]R. G. Shulman, S. Ogawa, and J. J. Hopfield, Arch. Biochem. Biophys. 151, 68 (1972).
[7]R. B. Shulman *et al.*, J. Mol. Biol. 53, 143 (1970).
[8]R. G. Shulman *et al.*, Science 165, 251 (1969).
[9]S. Ogawa, H. M. McConnell, and A. Horowitz, Proc. Natl. Acad. Sci. U. S. 61, 401 (1968).
[10]E. Antonini and M. Brunori, J. Biol. Chem. 244, 3909 (1969).
[11]M. F. Perutz, Nature 228, 726 (1970).
[12]J. J. Hopfield, J. Mol. Biol. 77, 207 (1973).
[13]D. Schooley, E. Bunnenberg, and C. Djerassi, Proc. Natl. Acad. Sci. U. S. 53, 579 (1965).
[14]V. E. Shashoua, Proc. Faraday Soc. 3, 61 (1969).
[15]R. Gale, A. J. McCaffery, and M. D. Rowe, J. Chem. Soc. Dalton Trans. 1972, 596.
[16]H. Rein, K. Ruckpaul, and W. Haberditzl, Chem. Phys. Lett. 20, 71 (1973).
[17]D. J. Caldwell and H. Eyring, J. Chem. Phys. 58, 1149 (1973).
[18]L. Vickery (private communication).
[19]B. Briat, D. Berger, and M. Leliboux, J. Chem. Phys. 57, 5606 (1972).
[20]S. Jasperson and S. E. Schnatterly, Rev. Sci. Instrum. 40, 761 (1969).
[21]A. B. Calender, Ph. D. thesis, Princeton University, 1970.
[22]J. I. Treu, A. B. Calender, and S. E. Schnatterly, Rev. Sci. Instrum. 44, 793 (1973).
[23]R. Benesch and G. Macduff, Anal. Biochem. 11, 81 (1965).
[24]J. I. Treu, Ph. D. thesis, Princeton University, 1973.
[25]E. Bucci and C. Fronticelli, J. Biol. Chem. 240, PC551 (1965).
[26]E. Antonini and M. Brunori, *Hemoglobin and Myoglobin in their Reactions with Ligands* (North-Holland, Amsterdam, 1971).
[27]W. T. Simpson, J. Chem. Phys. 17, 1218 (1949).
[28]H. C. Longuet-Higgins *et al.*, J. Chem. Phys. 18, 1174 (1950).
[29]M. Zener and M. Gouterman, Theoret. Chim. Acta (Berl.) 4, 44 (1966).
[30]M. Gouterman, J. Mol. Spectrosc. 6, 138 (1961).
[31]M. Gouterman, G. H. Wagniere, and L. C. Snyder, J. Mol. Spectrosc. 11, 108 (1963).
[32]C. Weiss, H. Kobayashi, and M. Gouterman, J. Mol. Spectrosc. 16, 415 (1965).
[33]M. Zerner and M. Gouterman, J. Chem. Phys. 30, 1139 (1959).
[34]M. H. Perrin, M. Gouterman, and C. L. Perrin, J. Chem. Phys. 50, 4137 (1969).
[35]M. Zerner, M. Gouterman, and H. Kobayashi, Theoret. Chim. Acta 6, 363 (1966).
[36]P. J. Stephens, W. Suetaak, and P. N. Schatz, J. Chem. Phys. 44, 4592 (1966).
[37]P. J. Stephens, J. Chem. Phys. 52, 3489 (1970).
[38]J. C. Sutherland *et al.*, J. Chem. Phys. 54, 2889 (1971).
[39]T. Spiro and T. Strekas, Proc. Natl. Acad. Sci. U. S. 69, 2622 (1972).
[40]M. Brunori, E. Antonini, J. Wyman, and S. Anderson, J. Mol. Biol. 34, 357 (1968).
[41]M. Malley and G. Feher, J. Mol. Spectrosc. 26, 320 (1968).
[42]M. Tinkham, *Group Theory and Quantum Mechanics* (McGraw-Hill, New York, 1964).